Langmuir

Article

pubs.acs.org/Langmuir

Using Optical Tweezers for the Characterization of Polyelectrolyte Solutions with Very Low Viscoelasticity

Angelo Pommella,*[,†,‡] Valentina Preziosi,[†,‡] Sergio Caserta,[†,‡,§] Jonathan M. Cooper,[∥] Stefano Guido,[†,‡,§] and Manlio Tassieri[∥]

[†]Dipartimento di Ingegneria Chimica, dei Materiali e della Produzione Industriale, Università di Napoli Federico II, P. le Tecchio 80, 80125 Napoli, Italy

[‡]CEINGE Advanced Biotechnologies, Via Gaetano Salvatore 486, 80145 Napoli, Italy

[§]Consorzio Interuniversitario Nazionale per la Scienza e Tecnologia dei Materiali (INSTM), UdR INSTM Napoli Federico II, P. le Tecchio, 80, 80125 Naples, Italy

[∥]Division of Biomedical Engineering, School of Engineering, University of Glasgow, Glasgow G12 8LT, U.K.

ABSTRACT: Recently, optical tweezing has been used to provide a method for microrheology addressed to measure the rheological properties of small volumes of samples. In this work, we corroborate this emerging field of microrheology by using these optical methods for the characterization of polyelectrolyte solutions with very low viscoelasticity. The influence of polyelectrolyte (i.e., polyacrylamide, PAM) concentration, specifically its aging, of the salt concentration is shown. The close agreement of the technique with classical bulk rheological measurements is demonstrated, illustrating the advantages of the technique.

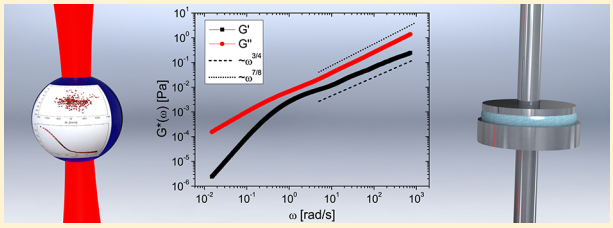

INTRODUCTION

The study of the rheological properties of polyelectrolytes, which in nature include nucleic acids, some proteins, and carbohydrates, has important consequences with respect to both an understanding of fundamental biological fluid dynamics and also emerging biotechnological applications.[1] Recent industrial examples of the use of either anionic or cationic synthetic polyelectrolytes[2] (carrying either negative or positive charges along their polymer chains) include applications in biomedical systems,[3] drug delivery,[4] the food industry,[5] water purification,[6] nanotechnology,[7,8] and surfactant solutions.[9,10]

In this context, polyacrylamide (PAM) is a commonly used polyelectrolyte, with applications that range from biology[11−13] to industries such as oil processing,[14] purification of natural water and wastewater,[15] and paper making.[16] Several literature studies concerning different methods for the preparation of polyacrylamide solutions[17−19] and the influence on their rheological properties of different parameters such as polymer concentration, solvent composition, temperature,[20−22] and aging of the sample have been reported.[23] In these cases, the rheological properties of PAM, in common with other water-based solutions of polyelectrolytes, are usually studied with conventional bulk rheometers[24] and can be described by means of frequency-dependent complex shear modulus $G^*(\omega) = G'(\omega) + iG''(\omega)$, where the real part (i.e., the elastic modulus $G'(\omega)$) provides a measure of the energy stored by the solution and the imaginary part (i.e., the viscous modulus $G''(\omega)$) provides a measure of the energy dissipated by the solution in response to the work exerted by an external force.

However, the measurement of these quantities becomes complicated at very low polyelectrolyte concentrations (i.e., a few parts per million). Under these circumstances, the rheological behavior of these solutions that have very weak viscoelasticity is not fully understood, in part because of the fact that the measurement of these systems often falls below the range of sensitivity of classical bulk rheometers. Thus, PAM solutions are rarely studied at polymer concentrations below 0.1%.[25] Notably, the weak elasticity of such fluids is of huge significance. For example, in multiphase systems these small interaction forces can strongly influence the emulsion morphology through the imposed flow as a result of the deformation,[26] break up, and coalescence[27] of the inclusions and through the formation of aggregates.[28] As a consequence, there is importance in understanding better these small interactions that occur in these low-concentration polyelectrolyte solutions by using more sensitive microrheological techniques.

In the past decade, many such microrheology techniques[29−43] have been developed and used to determine the rheological properties of viscoelastic fluids, including those involving the use of video particle tracking microrheology,[29] magnetic tweezers,[30] and dynamic light scattering.[31] Among these methods, the technique of optical tweezers, where a highly focused laser beam traps, in three dimensions,

Received: April 26, 2013
Revised: June 19, 2013
Published: June 20, 2013

   dx.doi.org/10.1021/la4015948 | *Langmuir* 2013, 29, 9224−9230

micrometer-sized dielectric particles suspended in a fluid,[32−34] has been extensively developed.[35−41] Most recently, a novel and simple analytical method for the analysis of optical tweezing data for microrheology has been proposed by Tassieri et al.,[42] greatly simplifying the application of the technique.

In this Article, we adopt this new method[42] to show the rheological characterization of very low concentration polyacrylamide solutions by means of optical tweezers measurements.[42] We compare these results to conventional rheology measurements, demonstrating the effectiveness of the technique in exploring the very weak interactions between these polyelectrolyte chains at low concentrations.[42] The sensitivity of the technique enables us not only to understand better the influence of polymer chain interactions but also to demonstrate the roles of salt concentration and aging in the rheological properties of these solutions.

THEORETICAL BACKGROUND

In optical tweezing, we consider the case of a micrometer-sized spherical particle suspended in a fluid at thermal equilibrium where it experiences random forces leading to Brownian motion, driven by the thermal fluctuations of the fluid's molecules. An analysis of the particle's trajectory reveals information on the viscoelastic properties of the suspending fluid, as demonstrated in the pioneering work of Mason and Weitz[43] that established the field of microrheology.

In the case when the probe's fluctuations are constrained by a stationary harmonic potential generated by optical tweezers, one could write a generalized Langevin equation

$$m\vec{a}(t) = \vec{f}_{\mathrm{R}}(t) - \int_0^t \zeta(t-\tau)\,\vec{v}(\tau)\,\mathrm{d}\tau - \kappa\vec{r}(t) \tag{1}$$

where m is the mass of the particle, $\vec{a}(t)$ is its acceleration, $\vec{v}(t)$ is its velocity, and $\vec{f}_{\mathrm{R}}(t)$ is the usual Gaussian white noise term, modeling stochastic thermal forces acting on the particle. The integral term, which incorporates a generalized time-dependent memory function, $\zeta(t)$, represents viscous damping by the fluid. Here, κ is the optical trap stiffness that can be easily determined by appealing to the principle of equipartition of energy

$$\frac{d}{2}k_{\mathrm{B}}T = \frac{1}{2}\kappa\langle r_j^2\rangle \tag{2}$$

where $\langle r_j^2\rangle$ is the time-independent variance of the Cartesian component ($j = x, y, z$) of the d-dimensional vector describing the particle's displacement from the trap center, the origin of $\vec{r}$.

It has been shown that eq 1 can be solved in terms of either the normalized mean-square displacement (NMSD) $\Pi(\tau) = \langle\Delta r^2(\tau)\rangle/2\langle r\rangle$[38] or the normalized position autocorrelation function (NPAF) $A(\tau) = \langle\vec{r}(t)\,\vec{r}(t+\tau)/r^2\rangle$[39]

$$G^*(\omega)\frac{6\pi a}{\kappa} = \left(\frac{1}{\mathrm{i}\omega\hat{\Pi}(\omega)} - 1\right) \equiv \left(\frac{1}{\mathrm{i}\omega\hat{A}(\omega)} - 1\right)^{-1} \tag{3}$$

where $\hat{\Pi}(\omega)$ and $\hat{A}(\omega)$ are the Fourier transforms of $\Pi(\tau)$ and $A(\tau)$, respectively. The inertia term ($m\omega^2$) reported in the original publications[38,39] can be neglected here because for micrometer-sized particles it becomes significant only above the megahertz frequency range.

Equation 3 relates the material's complex shear modulus $G^*(\omega)$ to the observed time-dependent bead trajectory $\vec{r}(t)$ via the Fourier transform of one of the related time-averaged quantities (i.e., $\Pi(\tau)$ or $A(\tau)$). The evaluation of these Fourier transforms, given only a finite set of data points over a finite time window, is performed by means of the analytical method recently proposed by Tassieri et al.[42]

EXPERIMENTAL SECTION

Materials. A 0.5 wt % stock polyacrylamide (PAM, M_w 7000 kDa, Dryfloc by SNF Italia) solution was made in distilled water (as the supporting solvent). Solutions were mixed for 48 h using magnetic stirrers at low speeds in order to prevent mechanical degradation of the polymer chains. The stock solution was then diluted by additions of distilled water in order to obtain final concentrations of 25, 50, 125, and 250 ppm (w/w). In this concentration range, the fluids show weak elasticity and a viscosity slightly higher than those of the solvent.[44] Sodium chloride (1, 2.5, and 5 wt %) was added to the final solutions to investigate the effect of salt on fluids rheology. To prevent degradation, the fluids were kept at 4 °C until the measurement was made.

Rheological Measurements. The rheological measurements on the sample were carried out at 20 °C by a stress-controlled rotational MCR 301 rheometer (Anton Paar Instruments) using double-gap geometry. A preshear[45] of 100 s^{-1} is applied for 60 s to cancel possible loading effects. The oscillatory tests are run in the range of linear viscoelasticity, as verified by preliminary amplitude sweep tests.

Microrheological Measurements. Optical trapping was achieved by means of a titanium−sapphire laser with a 5 W pump (Verdi V5 laser; Coherent Inc.), which provides up to 1 W at 830 nm. The tweezers use an inverted microscope, where the same objective lens (100×, 1.3 numerical aperture, Zeiss, Plan-Neofluar) both focuses the trapping beam and images the thermal fluctuations of a single 5-μm-diameter silica bead. Samples are mounted on a motorized microscope stage (Prior Pro-Scan II). A CMOS camera (Dalsa Genie HM640 GigE) was used to collect high-speed images of a reduced field of view. These images were processed in real time at ∼1 kHz using homemade LabVIEW (National Instruments) single-particle-tracking software[46] running on a personal computer. Note that each trajectory was made from at least 10^6 data points.

RESULTS

Figure 1 shows the normalized position autocorrelation function (NPAF) and the normalized mean-square displacement (NMSD) as a function of the lag time τ for a single optically trapped 5-μm-diameter silica bead suspended in two PAM solutions at concentrations of (a) 50 and (b) 250 ppm, respectively, with both containing 1 wt % NaCl. The inset of Figure 1a shows a 10 s part of the entire displacement of the bead along the x direction of the sample containing 50 ppm PAM. It is interesting that neither NPAF curve for these samples decays as a single exponential, as would be expected for a Newtonian fluid,[42] but instead shows an intermediate shoulder (or a plateau for the NMSD curves) before tending to zero (or to one in the case of the NMSDs). Such a shoulder (or plateau) is an interesting feature not previously observed for optical tweezers, although interestingly this has been predicted by a theoretical study of the dynamics of an optically trapped particle suspended in a Maxwell fluid.[47] This feature is related to the material's elastic plateau modulus, which constrains the bead fluctuations only temporarily. As described above, the fluids' linear viscoelastic properties (LVE) can be obtained from the analysis of the data shown in Figure 1 via eq 3.

In Figures 2 and 3, we show a comparison between microrheology, as measured by optical tweezers, and bulk rheology, measured using a rotational rheometer, for 50 and 250 ppm PAM with 1 wt % NaCl, the same fluids reported in Figure 1. In Figure 2, the elastic (G', circles) and viscous (G'', triangles) moduli are plotted as a function of the oscillation frequency for the two different techniques. The two method-

dx.doi.org/10.1021/la4015948 | Langmuir 2013, 29, 9224−9230

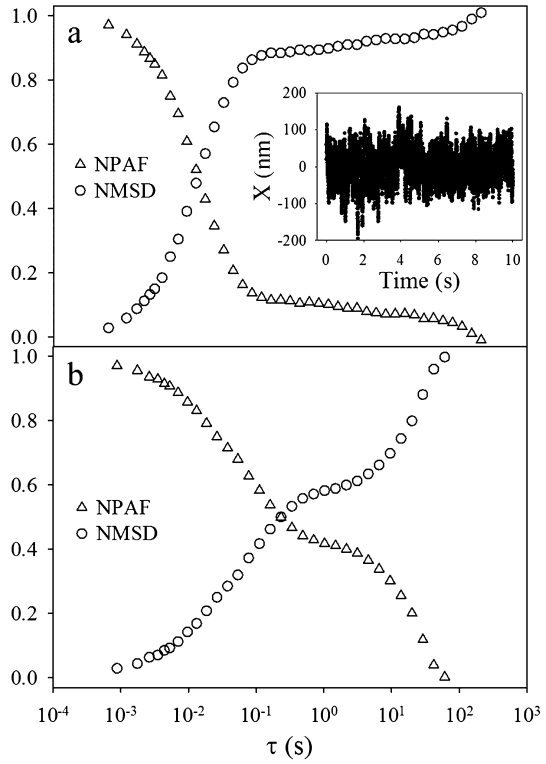

Figure 1. NPAF and NMSD vs delay time τ of a single optically trapped 5-μm-diameter silica bead suspended in two water-based solutions at PAM concentrations of (a) 50 and (b) 250 ppm with 1 wt % NaCl in both solutions. The inset of panel a shows a 10 s part of the entire displacement of the bead along the x direction.

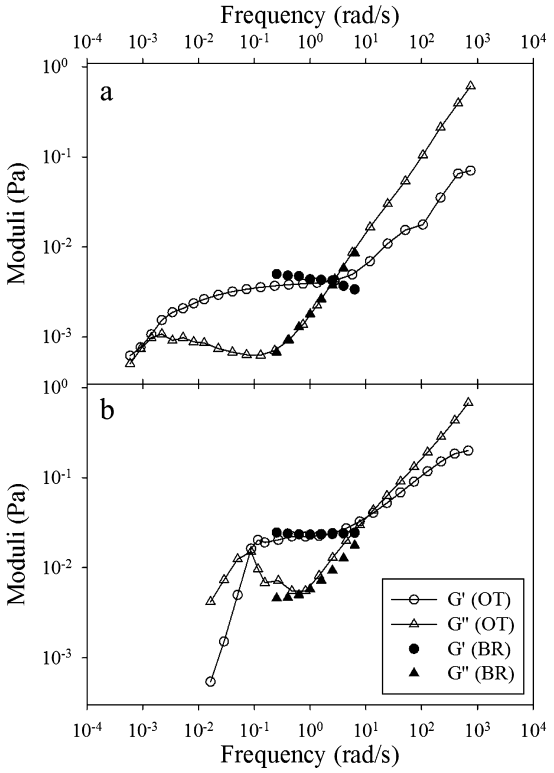

Figure 2. Elastic (G') and viscous (G'') moduli as a function of the oscillation frequency measured with optical tweezers (OT) and bulk rheometry (BR) are compared for (a) 50 and (b) 250 ppm PAM solutions with 1 wt % NaCl.

ologies show good agreement demonstrating that optical tweezing provides a precise measurement of the material LVE properties over a much wider range of frequencies, giving more information on the material characteristic relaxation times. It is interesting that both measurements provide for the two fluids the same estimation of the moduli slope and crossover frequency, with the latter being slightly higher for the 250 ppm solution (i.e., the crossover frequency is 2.8 rad/s for the 50 ppm sample and 11 rad/s for the 250 ppm sample).

In Figure 3, the same measurements are shown but instead the complex viscosity η^* is plotted against the frequency for both techniques (optical tweezing, circles; bulk rheology, triangles); η^* shows shear thinning trend down to a pseudo plateau value at frequencies higher than 10 rad/s, which is very close to the viscosity of water. At high frequencies, the solute molecules have no time to interact among each other, given the low concentration, and the fluid viscosity almost matches that of the solvent. In contrast, at low frequencies the viscosity increases, showing non-Newtonian behavior.

In Figure 3, the steady-shear viscosity (η), as measured using a bulk rotational rheometer, is also reported as a function of the shear rate and is compared to the two complex viscosity measurements; the excellent superimposition among the data indicates the applicability of the Cox–Merz empirical law.[48] The data are also in good agreement with previous measurements[44] on similar systems, reported only in the high-shear-rate range.

Figures 2 and 3 provide a quantitative validation of the microrheology measurements performed with optical tweezers in terms of both moduli and complex viscosity. In the analysis reported in this article, we use optical tweezers measurements to investigate the concentration functionality of the LVE properties of PAM solutions, the effects of salt (NaCl) addition and fluid aging.

Influence of PAM Concentration on LVE Properties. Figure 4 shows the concentration functionality of LVE properties for four different fluids with PAM concentration ranging from 25 to 250 ppm; measurements of the complex viscosity (η^*) and loss modulus (G'') for water are also reported for comparison. In Figure 4a, we report the elastic modulus G'. It can be seen that in the intermediate frequency range (ca. 10^{-1}–10 rad/s) G' shows a horizontal plateau, with the modulus being a growing function of the polymer concentration.

In contrast, the viscous modulus (G''), reported in Figure 4b, does not change substantially with the PAM concentration at high frequency. In the intermediate frequency range, some differences are still measurable. In this range, G''also shows a horizontal plateau, hence the horizontal trend in both moduli suggests a gel-like rheological behavior of the fluids in that frequency range.

Finally, the complex viscosity (η^*), calculated from the same measurement data, is reported in Figure 4c. In the low-frequency range, a significant increment is observed as a function of the PAM concentration, whereas at high frequencies all of the curves collapse to the same plateau, corresponding to the viscosity of water. In the thinning range of the complex viscosity plot, it was possible to estimate the power law index, n, from the data points' slope ($n - 1$). The measurements lead to the same value $n \approx 0.05$ for all of the PAM concentrations examined. A similar nondependency of n from the PAM concentration was previously observed in a different concen-

dx.doi.org/10.1021/la4015948 | Langmuir 2013, 29, 9224–9230

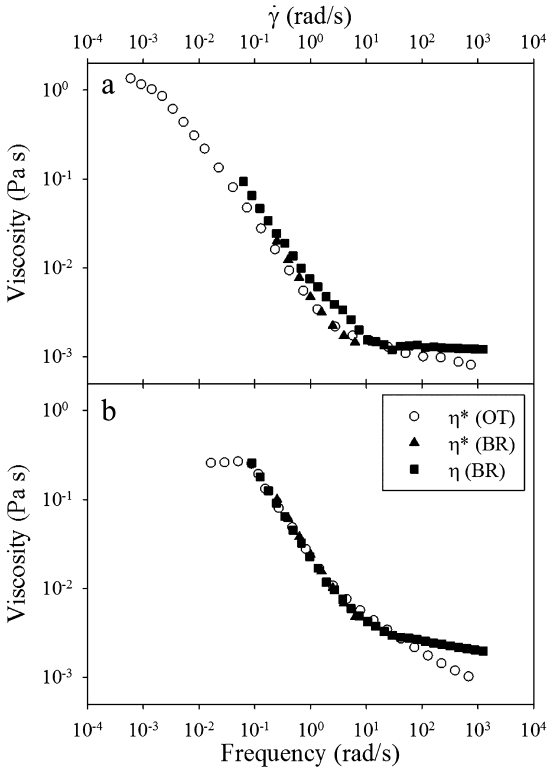

Figure 3. Frequency-dependent viscosity measured with optical tweezers and bulk rheometry, compared for (a) 50 and (b) 250 ppm PAM solutions with 1 wt % NaCl. Complex viscosities (η^*), plotted as a function of the frequency, are compared to shear viscosity (η), plotted as a function of the imposed shear rate ($\dot{\gamma}$), according to the Cox–Merz empirical law.

tration range, even if a higher value of n = 0.5 was reported.[25] The discrepancy can be likely attributed to different properties of the polyacrylamide samples used (i.e., molecular weight, degree of hydrolysis, and salt concentration). It is of note that the frequency where the fluids collapse to Newtonian behavior (i.e., the flow characteristic time when the PAM molecule interactions become negligible) occurs at higher frequencies as the PAM concentration increases, as expected. Overall we can state that the concentration functionality of the LVE properties of PAM solutions (Figure 4) is due to the increase in the number of entanglements between the PAM chains as shown in the literature.[25,49]

Further insight into the dependence of PAM concentration on fluid viscosity can be obtained by comparing viscosity values at a fixed frequency. We chose to compare data at ω = 0.15 rad/s (i.e., in the shear-thinning range, as indicated by the vertical line in Figure 4c). These viscosity values are plotted as a function of PAM concentration in Figure 5 where a nonlinear dependence ($\eta \approx c^{1.5}$) is shown. This dependence is typical of polyelectrolyte solutions in the semidilute entangled regime in a low-salt-concentration limit.[50]

Influence of Salt Concentration on the LVE Properties of PAM Solutions. In Figure 6, we report the effect of salt (NaCl) concentration on the LVE properties of a PAM solution at a concentration of 125 ppm. It can be seen that the elastic modulus of the PAM solution shows nonmonotonic behavior (Figure 6a) as a function of salt concentration. In fact, by adding 1 wt % sodium chloride to the solution an initial increment in the values of G' is observed, with the elastic

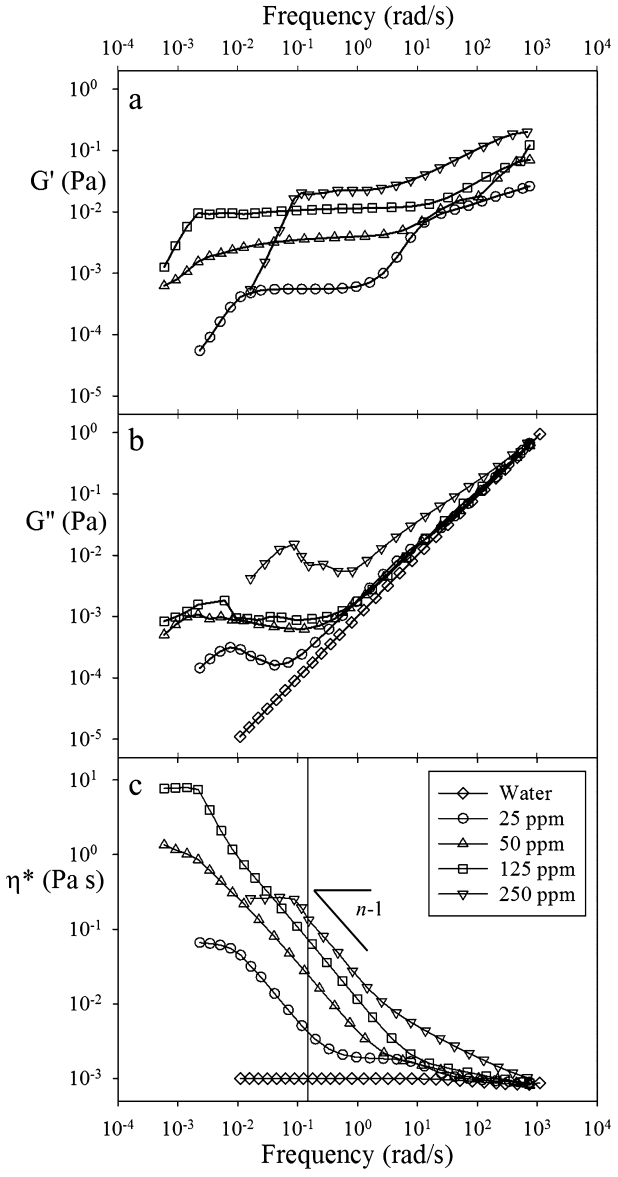

Figure 4. Concentration functionality of the linear viscoelastic properties ((a) G', (b) G'', and (c) the complex viscosity) of PAM solutions at concentrations of 25, 50, 125, and 250 ppm, respectively. All of the fluids have a NaCl concentration of 1 wt %.

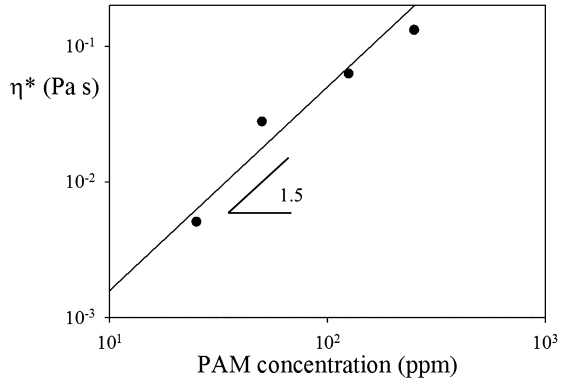

Figure 5. Complex viscosity evaluated at 0.15 rad/s vs PAM concentration. The continuous line is a guide for the gradient showing the prediction for the semidilute entangled regime of polyelectrolytes ($\eta \approx c^{1.5}$). A slope of 1.5 is reported as a reference.

dx.doi.org/10.1021/la4015948 | Langmuir 2013, 29, 9224–9230

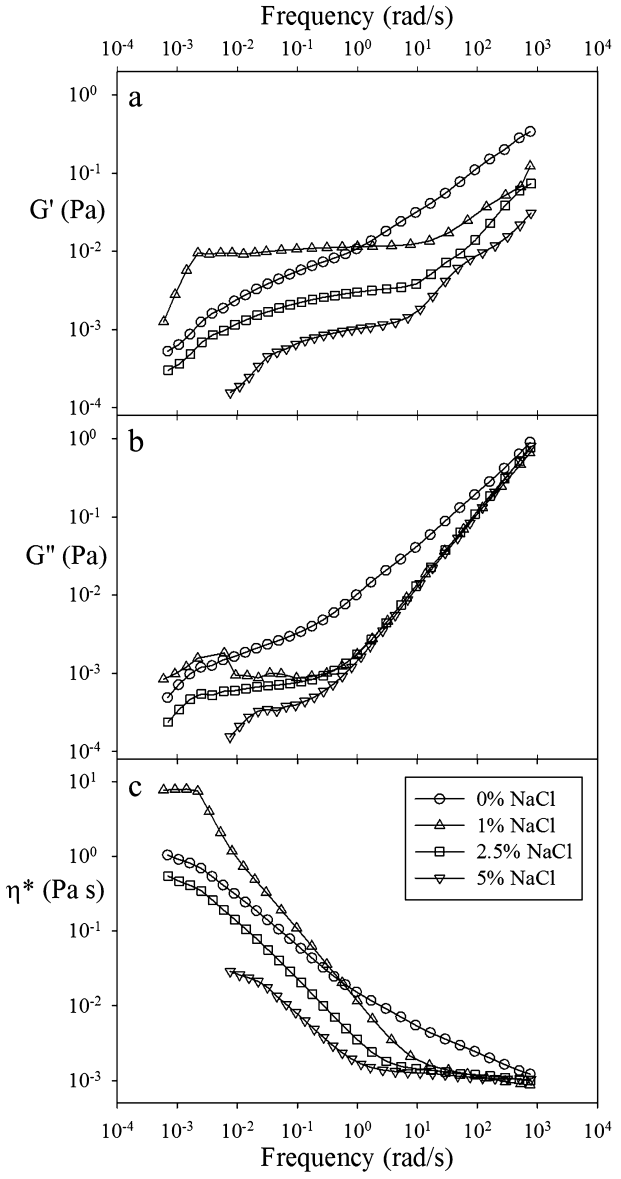

Figure 6. Viscoelastic moduli (a) G' and (b) G'' and (c) complex viscosity η^* vs frequency of a PAM solution at a concentration of 125 ppm for four different concentrations of salt (NaCl).

moduli showing a constant plateau for frequencies lower than 10 rad/s, whereas the further addition of salt causes a decrease in the G' value in the same range of frequencies. The viscous modulus (Figure 6b) shows a monotonic decrease in the low-frequency range, whereas at high frequencies all of the curves collapse together (with the exception for the no-salt fluid (0%) that presents higher values and a lower slope). The influence of the salt on the rheology is also reported in Figure 6c in terms of the complex viscosity, combining the data of the two moduli.

This nonmonotonic effect of salt concentration on G' is possibly due to salt effects on the inter- and intramolecular charges. When a polyelectrolyte is dissolved in water in the absence of salt, the chain swells because of the mutual repulsion of internal charges (negative in our polyacrylamide samples) in order to minimize the electric intramolecular interactions. This same mechanism hinders intermolecular interactions between chains at these very low values of PAM concentration; this interpretation is consistent with the fact that the sample without salt does not show any gel-like behavior over the entire frequency range investigated (Figure 6).

We observe that by adding a small amount of NaCl (1 wt %) gel-like behavior is exhibited (Figure 6). This is due to the fact that salt ions shield all intra- and intermolecular electric interactions between and within the chains. Such shielding of charges favors the interaction between different chains, whereas it causes chain shrinkage on the intramolecular level. Thus, we conclude that at low salt concentration the chain shrinkage is not sufficient to prevent intermolecular interactions, thus allowing the gel-like behavior that is found in the middle frequency range investigated (Figure 6). In this scenario, further addition of salt generates a stronger shrinkage of the PAM chains with a consequent decrease in the value of G' resulting from the decrease in the number of entanglements among the chains. Similar weakening in G' due to the addition of salt has already been observed in PAM gels.[51,52]

Aging Effect on the LVE Properties of PAM Solutions. In Figure 7, we report the changes, measured over 5 weeks, of the viscoelastic properties of a PAM solution at a concentration of 125 ppm with 1 wt % NaCl. It is clear that there is a considerable drop in the viscoelastic properties within the first 3 weeks of sample preparation. Once again, the main effect is measured for the elastic modulus (G'), as reported in Figure 7a, and is also reflected in terms of the complex viscosity (η^*), as reported in Figure 7c, whereas the viscous modulus (G'') shows only limited changes, mainly at low frequencies (Figure 7b).

After a period of about 3 weeks, the aging appears not to affect additional LVE properties, and the measurements were consistently reproducible. The effect of aging on PAM solutions was previously attributed to the weakness of the entanglements between the PAM chains.[23] These interactions, unlike the stronger covalent bonds, could change with time and modify the internal structure of the samples until some equilibrium is eventually reached.

■ CONCLUSIONS

A rheological characterization of polyacrylamide solutions with very low viscoelasticity was carried out both by optical tweezers and bulk rheology. Remarkable agreement between these two techniques was found. Hence, we demonstrate the validity of the optical tweezers as a tool for the rheological characterization of weakly viscoelastic polyelectrolyte solutions. This technique allows the investigation of much lower values of the elastic modulus (below 10^{-3} Pa) over a wider range of frequency when compared to classical bulk rheological measurements.

Furthermore, the concentration dependency of the linear viscoelastic properties of PAM solutions was studied, and good agreement with literature data was found. Finally, we have investigated the influence of the addition of salt and aging on the linear viscoelastic properties of a PAM solution. A nonmonotonic salt influence on very low concentration PAM solutions was found, depending on the salt concentration; indeed, the addition of salt can generate weak gel-like behavior at first whereas further salt addition appears to weaken any PAM network. We also showed that PAM samples change with time after preparation and need at least 3 weeks to reach a stationary morphology. These results are relevant to the characterization of polyelectrolyte solutions with very low polymer concentrations, with applications in the food, detergent, and pharmaceutical industries, where polyelectrolytes are used to improve product stability and rheology.

dx.doi.org/10.1021/la4015948 | Langmuir 2013, 29, 9224−9230

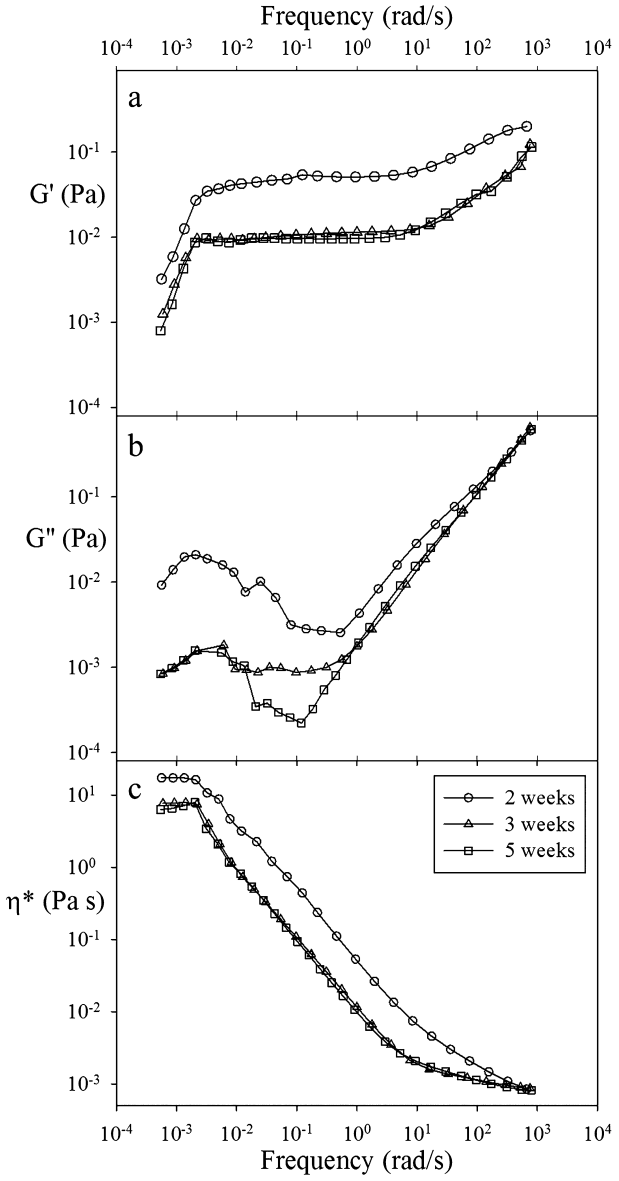

Figure 7. Aging of the viscoelastic properties of a PAM solution at a concentration of 125 ppm and with 1 wt % NaCl.

AUTHOR INFORMATION

Corresponding Author

*E-mail: angelo.pommella@gmail.com.

Notes

The authors declare no competing financial interest.

ACKNOWLEDGMENTS

This study is related to the activity of European network action COST MP1106 "Smart and green interfaces - from single bubbles and drops to industrial, environmental and biomedical applications". M.T. acknowledges support via a personal research fellowship from the Royal Academy of Engineering/EPSRC. We thank Niall P. Macdonald for contributions to this work.

REFERENCES

(1) Tripathy, S. K.; Kumar, J.; Nalwa, H. S. *Handbook of Polyelectrolytes and Their Applications: Polyelectrolytes, Their Characterization and Polyelectrolye Solutions*; American Scientific Publishers: Stevenson Ranch, CA, 2002.

(2) Mortimer, D. A. Synthetic Polyelectrolytes—A Review. *Polym. Int.* **1991**, *25*, 29−41.

(3) Peppas, N.; Langer, R.; Scranton, A. B.; Rangarajan, B.; Klier, J. *Biopolymers II*; Springer: Berlin, 1995; Vol. *122*, pp 1−54.

(4) Lankalapalli, S.; Kolapalli, V. R. M. Polyelectrolyte Complexes: A Review of their Applicability in Drug Delivery Technology. *Indian J. Pharm. Sci.* **2009**, *71*, 481−487.

(5) Simeone, M.; Alfani, A.; Guido, S. *Phase Diagram, Rheology and Interfacial Tension of Aqueous Mixtures of Na-Caseinate and Na-Alginate Food Hydrocolloids* **2004**, *18*, 463−470.

(6) Raymond, S. F. *Polyelectrolytes and Polyzwitterions*; American Chemical Society: Washington, DC, 2006; Vol. *937*, pp 153−168.

(7) Sun, B.; Mutch, S. A.; Lorenz, R. M.; Chiu, D. T. Layered Polyelectrolyte-Silica Coating for Nanocapsules. *Langmuir* **2005**, *21*, 10763−10769.

(8) Carrillo, J.-M. Y.; Dobrynin, A. V. Layer-by-Layer Assembly of Polyelectrolyte Chains and Nanoparticles on Nanoporous Substrates: Molecular Dynamics Simulations. *Langmuir* **2011**, *28*, 1531−1538.

(9) Dedinaite, A.; Claesson, P. M.; Bergström, M. Polyelectrolyte−Surfactant Layers: Adsorption of Preformed Aggregates versus Adsorption of Surfactant to Preadsorbed Polyelectrolyte. *Langmuir* **2000**, *16*, 5257−5266.

(10) Wallin, T.; Linse, P. Polyelectrolyte-Induced Micellization of Charged Surfactants. Calculations Based on a Self-Consistent Field Lattice Model. *Langmuir* **1998**, *14*, 2940−2949.

(11) Zangmeister, R. A.; Tarlov, M. J. UV Graft Polymerization of Polyacrylamide Hydrogel Plugs in Microfluidic Channels. *Langmuir* **2003**, *19*, 6901−6904.

(12) Schägger, H.; von Jagow, G. Tricine-Sodium Dodecyl Sulfate-Polyacrylamide Gel Electrophoresis for the Separation of Proteins in the Range from 1 to 100 kDa. *Anal. Biochem.* **1987**, *166*, 368−379.

(13) Rosiak, J.; Burozak, K.; Pękala, W. Polyacrylamide Hydrogels As Sustained Release Drug Delivery Dressing Materials. *Radiat. Phys. Chem.* **1983**, *22*, 907−915.

(14) Sokker, H. H.; El-Sawy, N. M.; Hassan, M. A.; El-Anadouli, B. E. Adsorption of Crude Oil from Aqueous Solution by Hydrogel of Chitosan Based Polyacrylamide Prepared by Radiation Induced Graft Polymerization. *J. Hazard. Mater.* **2011**, *190*, 359−365.

(15) Kurenkov, V. F.; Hartan, H.-G.; Lobanov, F. I. Application of Polyacrylamide Flocculants for Water Treatment. Chemistry and Computational Simulations. *Butlerov Commun.* **2002**, *3*, 31−40.

(16) Lu, S.; Liu, R.; Sun, X. A Study on the Synthesis and Application of an Inverse Emulsion of Amphoteric Polyacrylamide As a Retention Aid in Papermaking. *J. Appl. Polym. Sci.* **2002**, *84*, 343−350.

(17) Philippova, O. E.; Rulkens, R.; Kovtunenko, B. I.; Abramchuk, S. S.; Khokhlov, A. R.; Wegner, G. Polyacrylamide Hydrogels with Trapped Polyelectrolyte Rods. *Macromolecules* **1998**, *31*, 1168−1179.

(18) Mayer, C. R.; Thouvenot, R.; Lalot, T. Hybrid Hydrogels Obtained by the Copolymerization of Acrylamide with Aggregates of Methacryloyl Derivatives of Polyoxotungstates. A Comparison with Polyacrylamide Hydrogels with Trapped Aggregates. *Macromolecules* **2000**, *33*, 4433−4437.

(19) Muniz, E. C.; Geuskens, G. Compressive Elastic Modulus of Polyacrylamide Hydrogels and Semi-IPNs with Poly(N-isopropylacrylamide). *Macromolecules* **2001**, *34*, 4480−4484.

(20) Hu, Y.; Wang, S. Q.; Jamieson, A. M. Rheological and Rheooptical Studies of Shear-Thickening Polyacrylamide Solutions. *Macromolecules* **1995**, *28*, 1847−1853.

(21) Samchenko, Y. M.; Ul'berg, Z. R.; Komarskii, S. A.; Kovzun, I. G.; Protsenko, I. T. Rheological Properties of Acrylamide Hydrogels. *Colloid J.* **2004**, *66*, 350−354.

(22) Shevchenko, T. V.; Ul'rikh, E. V.; Yakovchenko, M. A.; Pirogov, A. N.; Smirnov, O. E. Rheological Properties of Polyacrylamide-Based Hydrogels. *Colloid J.* **2004**, *66*, 756−759.

(23) Ilavsky, M.; Hrouz, J.; Stejskal, J.; Bouchal, K. Phase Transition in Swollen Gels. 6. Effect of Aging on the Extent of Hydrolysis of

Aqueous Polyacrylamide Solutions and on the Collapse of Gels. *Macromolecules* **1984**, *17*, 2868−2874.
(24) Larson, R. G. *The Structure and Rheology of Complex Fluids*; Oxford University Press: Oxford, U.K., 1999.
(25) Ghannam, M. T.; Esmail, M. N. Rheological Properties of Aqueous Polyacrylamide Solutions. *J. Appl. Polym. Sci.* **1998**, *69*, 1587−1597.
(26) Pommella, A.; Caserta, S.; Guida, V.; Guido, S. Shear-Induced Deformation of Surfactant Multilamellar Vesicles. *Phys. Rev. Lett.* **2012**, *108*, 138301.
(27) Caserta, S.; Simeone, M.; Guido, S. Evolution of Drop Size Distribution of Polymer Blends under Shear Flow by Optical Sectioning. *Rheol. Acta* **2004**, *43*, 491−501.
(28) Caserta, S.; Simeone, M.; Guido, S. Shear Banding in Biphasic Liquid-Liquid Systems. *Phys. Rev. Lett.* **2008**, *100*, 137801.
(29) Van den Ende, D.; Purnomo, E. H.; Duits, M. H. G.; Richtering, W.; Mugele, F. Aging in Dense Suspensions of Soft Thermosensitive Microgel Particles Studied with Particle-Tracking Microrheology. *Phys. Rev. E* **2010**, *81*, 011404.
(30) Tassieri, M.; Evans, R. M. L.; Waigh, T. A.; Trinick, J.; Aggeli, A. Analysis of the Linear Viscoelasticity of Polyelectrolytes by Magnetic Microrheometry — Pulsed Creep Experiments and the One Particle Response. *J. Rheol.* **2010**, *54*, 117−131.
(31) Golan, S.; Talmon, Y. Nanostructure of Complexes between Cationic Lipids and an Oppositely Charged Polyelectrolyte. *Langmuir* **2012**, *28*, 1668−1672.
(32) Ashkin, A. Acceleration and Trapping of Particles by Radiation Pressure. *Phys. Rev. Lett.* **1970**, *24*, 156−159.
(33) Ashkin, A.; Dziedzic, J. M. Optical Levitation by Radiation Pressure. *Appl. Phys. Lett.* **1971**, *19*, 283−285.
(34) Ashkin, A.; Dziedzic, J. M.; Bjorkholm, J. E.; Chu, S. Observation of a Single-Beam Gradient Force Optical Trap for Dielectric Particles. *Opt. Lett.* **1986**, *11*, 288−290.
(35) Brau, R. R.; Ferrer, J. M.; Lee, H.; Castro, C. E.; Tam, B. K.; Tarsa, P. B.; Matsudaira, P.; Boyce, M. C.; Kamm, R. D.; Lang, M. J. Passive and Active Microrheology with Optical Tweezers. *J. Opt. A: Pure Appl. Opt.* **2007**, *9*, S103.
(36) Fischer, M.; Berg-Sørensen, K. Calibration of Trapping Force and Response Function of Optical Tweezers in Viscoelastic Media. *J. Opt. A: Pure Appl. Opt.* **2007**, *9*, S239.
(37) Atakhorrami, M.; Sulkowska, J. I.; Addas, K. M.; Koenderink, G. H.; Tang, J. X.; Levine, A. J.; MacKintosh, F. C.; Schmidt, C. F. Correlated Fluctuations of Microparticles in Viscoelastic Solutions: Quantitative Measurement of Material Properties by Microrheology in the Presence of Optical Traps. *Phys. Rev. E* **2006**, *73*, 061501.
(38) Tassieri, M.; Gibson, G. M.; Evans, R. M. L.; Yao, A. M.; Warren, R.; Padgett, M. J.; Cooper, J. M. Measuring Storage and Loss Moduli Using Optical Tweezers: Broadband Microrheology. *Phys. Rev. E* **2010**, *81*, 026308.
(39) Preece, D.; Warren, R.; Evans, R. M. L.; Gibson, G. M.; Padgett, M. J.; Cooper, J. M.; Tassieri, M. Optical Tweezers: Wideband Microrheology. *J. Opt.* **2011**, *13*, 044022.
(40) Valentine, M. T.; Dewalt, L. E.; Ou-Yang, H. D. Forces on a Colloidal Particle in a Polymer Solution: A Study Using Optical Tweezers. *J. Phys.: Condens. Matter* **1996**, *8*, 9477.
(41) Starrs, L.; Bartlett, P. One- and Two-Point Micro-Rheology of Viscoelastic Media. *J. Phys.: Condens. Matter* **2003**, *15*, S251.
(42) Tassieri, M.; Evans, R. M. L.; Warren, R. L.; Bailey, N. J.; Cooper, J. M. Microrheology with Optical Tweezers: Data analysis. *New J. Phys.* **2012**, *14*, 115032.
(43) Mason, T. G.; Weitz, D. A. Optical Measurements of Frequency-Dependent Linear Viscoelastic Moduli of Complex Fluids. *Phys. Rev. Lett.* **1995**, *74*, 1250−1253.
(44) Campo-Deaño, L.; Galindo-Rosales, F. J.; Pinho, F. T.; Alves, M. A.; Oliveira, M. S. N. Flow of Low Viscosity Boger Fluids through a Microfluidic Hyperbolic Contraction. *J. Non-Newton. Fluid* **2011**, *166*, 1286−1296.
(45) Caserta, S.; Guido, S. Vorticity Banding in Biphasic Polymer Blends. *Langmuir* **2012**, *28*, 16254−16262.
(46) Gibson, G. M.; Leach, J.; Keen, S.; Wright, A. J.; Padgett, M. J. Measuring the Accuracy of Particle Position and Force in Optical Tweezers Using High-Speed Video Microscopy. *Opt. Express* **2008**, *16*, 14561−14570.
(47) Grimm, M.; Jeney, S.; Franosch, T. Brownian Motion in a Maxwell Fluid. *Soft Matter* **2011**, *7*, 2076−2084.
(48) Cox, W. P.; Merz, E. H. Correlation of Dynamic and Steady Flow Viscosities. *J. Polym. Sci.* **1958**, *28*, 619−622.
(49) Yang, M.-H. The Rheological Behavior of Polyacrylamide Solution. *J. Polym. Eng.* **1999**, *19*, 371−381.
(50) Dobrynin, A. V.; Colby, R. H.; Rubinstein, M. Scaling Theory of Polyelectrolyte Solutions. *Macromolecules* **1995**, *28*, 1859−1871.
(51) Tam, K. C.; Tiu, C. Role of Ionic Species and Valency on the Steady Shear Behavior of Partially Hydrolyzed Polyacrylamide Solutions. *Colloid Polym. Sci.* **1990**, *268*, 911−920.
(52) Jar, P. Y. B.; Wu, Y. S. Effect of Counter-Ions on Swelling and Shrinkage of Polyacrylamide-Based Ionic Gels. *Polymer* **1997**, *38*, 2557−2560.